ARL-TR-9133 ● Dec 2020

DEVCOM ARMY RESEARCH LABORATORY

Additive Manufacturing of Boron Carbide by Direct-Ink Write (DIW)

by Nicholas Ku, Brennan Gray, Joshua Pelz, Kris Behler, Jerry LaSalvia, and Lionel Vargas-Gonzalez

NOTICES

Disclaimers

The findings in this report are not to be construed as an official Department of the Army position unless so designated by other authorized documents.

Citation of manufacturer's or trade names does not constitute an official endorsement or approval of the use thereof.

Destroy this report when it is no longer needed. Do not return it to the originator.

ARL-TR-9133 ● DEC 2020

Additive Manufacturing of Boron Carbide by Direct-Ink Write (DIW)

Nicholas Ku, Kris Behler, Jerry LaSalvia, and Lionel Vargas-Gonzalez
Weapons and Materials Research Directorate, DEVCOM Army Research Laboratory

Brennan Gray
College Qualified Leaders Program, University of Maryland, College Park

Joshua Pelz
Oak Ridge Associated Universities

REPORT DOCUMENTATION PAGE

Form Approved
OMB No. 0704-0188

1. REPORT DATE *(DD-MM-YYYY)*	2. REPORT TYPE	3. DATES COVERED (From - To)
December 2020	Technical Report	September 2018–January 2020

4. TITLE AND SUBTITLE
Additive Manufacturing of Boron Carbide by Direct-Ink Write (DIW)

5a. CONTRACT NUMBER

5b. GRANT NUMBER

5c. PROGRAM ELEMENT NUMBER

6. AUTHOR(S)
Nicholas Ku, Brennan Gray, Joshua Pelz, Kris Behler, Jerry LaSalvia, and Lionel Vargas-Gonzalez

5d. PROJECT NUMBER

5e. TASK NUMBER

5f. WORK UNIT NUMBER

7. PERFORMING ORGANIZATION NAME(S) AND ADDRESS(ES)
DEVCOM Army Research Laboratory
ATTN: FCDD-RLW-ME
Aberdeen Proving Ground, MD 21005

8. PERFORMING ORGANIZATION REPORT NUMBER
ARL-TR-9133

9. SPONSORING/MONITORING AGENCY NAME(S) AND ADDRESS(ES)

10. SPONSOR/MONITOR'S ACRONYM(S)

11. SPONSOR/MONITOR'S REPORT NUMBER(S)

12. DISTRIBUTION/AVAILABILITY STATEMENT
Approved for public release; distribution is unlimited.

13. SUPPLEMENTARY NOTES
ORCID ID(s): Nicholas Ku, 0000-0002-1276-4927; Kris Behler, 0000-0002-0579-1732; Lionel Vargas-Gonzalez, 0000-0001-6500-1686

14. ABSTRACT
Direct-ink writing (DIW) is an additive manufacturing method that enables on-demand "printing" of materials into multiscale complex structures for rapid prototyping and near-net-shape manufacturing. One of the challenges of using DIW for creating ceramic green bodies is to optimize the rheological properties of the ceramic-filled suspensions or "inks" to ensure stable flow within the printer apparatus, minimal distortion of the printed body due to gravity (referred to as "slumping"), and minimal defects. The purpose of this research is to develop boron carbide (B_4C) suspensions with optimal rheological properties suitable for DIW, as well as to understand the effect of the process on the bulk mechanical properties of the resulting printed and densified body. The effects of B_4C content, methylcellulose binder variation, and binder content on the rheological properties of B_4C suspensions were tested on a rotational rheometer to determine viscosity as a function of shear stress, as well as yield stress values, in an effort to identify an optimal suspension composition for printing. Subsequently, printed green bodies underwent a binder burnout step to remove the organic binder, and then were consolidated to high density via pressureless sintering. Microstructure and Knoop hardness were characterized. Theoretical densities as high 94.35% and Knoop hardness values of 19.24 GPa were achieved in the samples.

15. SUBJECT TERMS
ceramics processing, rheology, additive manufacturing, boron carbide, 3D printing

16. SECURITY CLASSIFICATION OF:			17. LIMITATION OF ABSTRACT	18. NUMBER OF PAGES	19a. NAME OF RESPONSIBLE PERSON
a. REPORT	b. ABSTRACT	c. THIS PAGE			Nicholas Ku
Unclassified	Unclassified	Unclassified	UU	26	19b. TELEPHONE NUMBER (Include area code) (410) 306-4592

Contents

List of Figures

Acknowledgments

The researchers would like to the thank Steve Kilczewski and William Gamble for their technical input and assistance, respectively.

This research was sponsored by the US DEVCOM Army Research Laboratory and was accomplished under Cooperative Agreement Number W911NF-19-2-0054 and W911NF-16-2-0050-P0003.

1. Introduction

Boron carbide (nominally B_4C) is a ceramic material with a high hardness, low density, high melting point, and low chemical reactivity, making it ideal for structural, thermal, and tribological applications.[1] In terms of performance, B_4C has historically been one of the most promising monolithic ceramic materials used in lightweight impact-resistant systems, despite its relatively high cost compared to other traditional structural ceramics.[2] Commercially available B_4C is generally manufactured via uniaxial hot pressing, which limits the ability to fabricate complex shapes. Research on pressureless sintering with post–hot isostatic pressing (HIP) of B_4C has resulted in densities near 96% of theoretical density (TD) and properties nearly equivalent to B_4C densified by pressure-assisted methods.[3] Combined with a near-net-shape forming method, this could lead to a reduction in postprocessing procedures of complex-shaped B_4C parts, such as cost-intensive machining.

The emerging technology of additive manufacturing (AM) enables the processing of ceramic parts with complex geometries.[4,5] This method has been highlighted as a means to enable near-net-shape manufacturing of conformal parts.[6] Furthermore, AM facilitates mesoscale tailoring, which could improve mechanical performance over monolithic ceramics.[7,8] Examples of mesoscale tailoring include functional grading of the composition and printing of biomimetic structures.[7] Recent work has been aimed at developing the processing science to form such structures through AM.[8–10]

The three most common ceramic AM approaches are vat photopolymerization, powder bed fusion, and material extrusion. All three methods are defined as indirect AM processes, as the printing process produces a particulate green body. Unlike metal or polymer AM processes, such as direct metal laser sinter or fused deposition modelling where the printing process produces the final product, indirect ceramic AM processes produce an intermediate product where further processing is required to turn it into the final product.[11] The traditional process steps for a carbide ceramic are shown in Fig. 1, with the alternate route shown for AM processes as a replacement to the usual forming techniques.

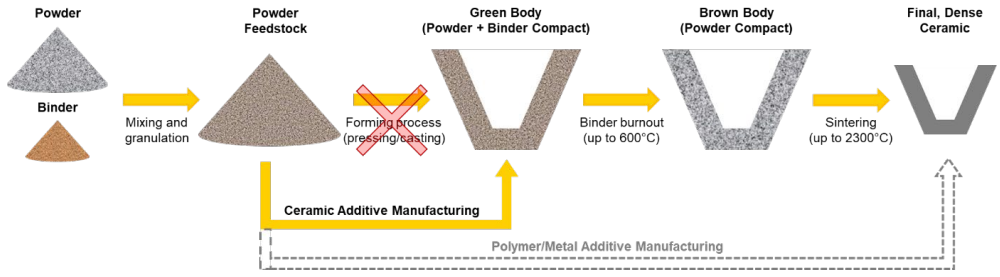

Fig. 1 General ceramic processing steps

The ceramic AM vat photopolymerization process, commonly termed stereolithography, relies on ceramic powder being dispersed in a liquid resin, which can be cured using a light source. The particulate-loaded resin is preferentially cured layer by layer to form the part. For the process to work, the light source, typically in the ultraviolet (UV) wavelength regime, must be able to penetrate through the particulate-loaded resin in order to cure the resin.[12] This is challenging for B_4C, which has a much higher refractive index mismatch than most oxide-loaded systems. This, in turn, leads to scattering and reduced penetration depth of the UV light, thereby reducing the layer thickness and increasing build times.

Powder bed fusion methods rely on a liquid binder system or thermal sintering process to locally fuse particles in a powder bed. By spreading more powder iteratively over the print area between fusing the particles, complex shapes can be formed within the powder bed layer by layer. The primary challenge to this approach is achieving a high enough packing density (i.e., green density) to be sintered to full density.[13] Because porosity within the final ceramic can be detrimental to bulk mechanical performance, powder bed fusion may be ill-suited for additively manufacturing structural ceramics, with the exception of those whose powders can be packed to densities greater than 60% theoretical density.

Direct-ink write (DIW) is the broad term for any extrusion-type process where material is deposited by a nozzle in traces, layer by layer. The material is then self-supported via cooling, gelation, or other rheological effects.[14] DIW is not a new process; the method of depositing a particulate-loaded suspension or slurry was originally called robocasting.[15] Since a requirement for a fully dense ceramic part is a high green density, the primary challenge for the DIW approach has been formulating ceramic suspensions that possess the desired rheological behavior. The suspension must have a high enough solids loading to form a part with a high green density, yet it cannot exceed the critical solids loading for dilatancy, or shear thickening, which prevents stable flow during extrusion.[16]

Stable flow in the ceramic suspension during the extrusion process is necessary for printing green bodies with minimal dimensional variations and defects. Thus, rheological behavior is an important factor when determining whether a suspension can be processed by DIW. Particulate-loaded suspensions act as non-Newtonian fluids, with five different types of behaviors shown in Fig. 2A.[17] The ideal rheology for a DIW suspension is a yield-pseudoplastic behavior,[18] also called a shear-thinning behavior, where the apparent viscosity of the system is high at low shear rates and low at high shear rates. This facilitates flow at high shear rates during extrusion through a nozzle, but then allows for high viscosity when the shear is removed to prevent slumping of the material after deposition. Yield-pseudoplastic behavior can be enhanced by causing the particles to flocculate, or encourage

adhesion between particles, with the breakdown of the particle network shown in Fig. 2B. Conversely, dilatant flow, which occurs when particle collisions dominate during shear flow and requires the local structure to expand to facilitate movement of the particles (as shown in Fig. 2C), must be avoided. These collisions increase with powder loading and shear rate.[17] Dudukovic et al. measured viscosity as a function of shear rate for various suspension compositions to characterize suspensions as a means to develop material formulations for a DIW process.[19]

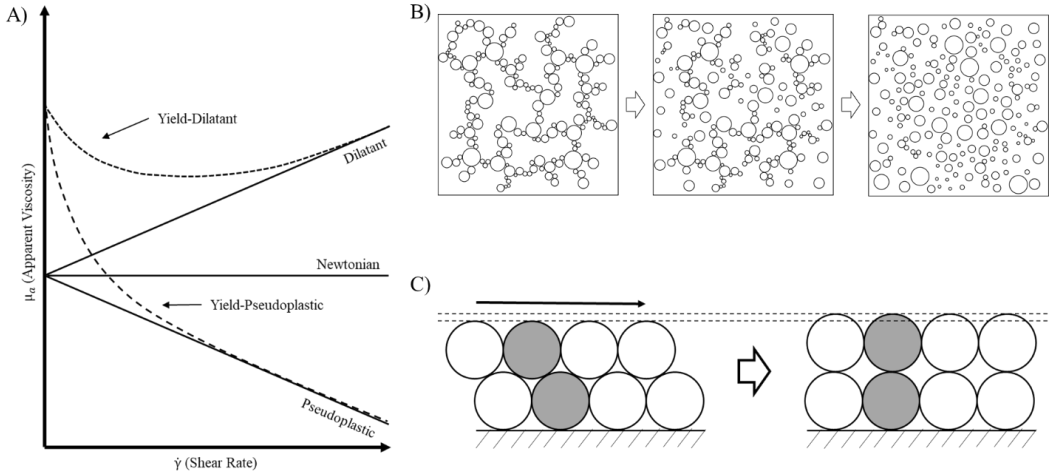

Fig. 2 Idealized rheological behaviors of non-Newtonian fluids A) plotted apparent viscosity as a function of shear rate. Schematic illustrations showing B) a shear-thinning process and C) a shear-thickening dilatant reaction to shear.

To gain insight into the "yield" viscosity of a suspension, the viscoelasticity of the suspension must be quantified. Shown in Fig. 3, a viscoelastic material will act as an elastic body with a dominant storage modulus until a critical flow stress is exceeded, at which point the material has yielded and behaves as a fluid with a dominant loss modulus.[20] For the DIW process, a stiffer suspension with higher values for both the storage modulus and flow stress would be desirable. M'barki et al. identified the modulus profile of the suspension as a key metric for printability and part stability in DIW suspension development.[21]

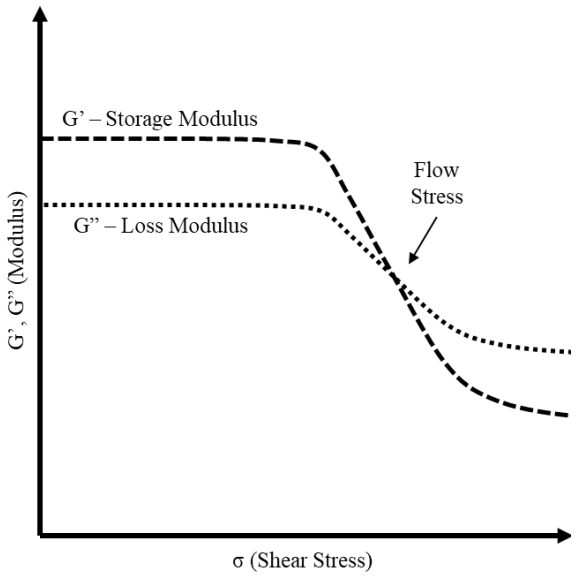

Fig. 3 Example plot of the shear moduli of a viscoelastic fluid as a function of shear stress

Recent work has shown the ability to DIW aluminum oxide,[22] silicon nitride,[23] and silicon carbide [24] suspensions with a high solids loading and subsequently sinter them to high densities. Costakis et al.[25] successfully developed B_4C suspensions with 54 vol% solids loading. Pressureless sintering of printed parts at 2000 °C without sintering aids yielded a density of only 82% TD. Sintering at higher temperatures and use of sintering aids can increase part density.[26] Additionally, increasing the solids loading of the suspension may aid in increasing the sintered density, although it comes with increased rheological challenges. Recent advancements in DIW printer designs have shown that using an auger-assisted print head can aid in the shear and conveyance of the material within the nozzle to extrude more viscous suspensions.[9] Furthermore, work by Cai et al.[24] has shown the advantage of using methylcellulose (MC) as a rheological modifier in highly particulate-loaded silicon carbide suspensions for DIW. The MC was found to act as a viscosifying agent, enhancing shear-thinning behavior as well as preventing phase separation during extrusion.[24]

Qualification of AM parts has been a major challenge for the technology to overcome and be adopted in many applications. This is no different for structural ceramics, with recent work finding AM process-related defects causing poorer performance compared to traditionally processed materials in dynamic impact testing.[6,27] In the ceramics community, hardness has traditionally been accepted as one of the most relevant mechanical properties to indicate good impact-related performance.[28] For example, CoorsTek* pressure-assisted densified (PAD) B_4C is

* CoorsTek Vista, Vista, CA 92081

a commercially available ceramic that has a listed Knoop hardness of 25.5 GPa at 1-kg load, which is significantly higher than most oxide ceramics.

In this report, B_4C suspensions were formulated for DIW. The effects of ceramic solids loading and MC content on flow behavior were investigated; rheometer measurements were coupled with empirical observations of printing performance. Additionally, suspensions were printed into green bodies and densified by pressureless sintering at several temperatures to determine the effects of sintering temperature on densification. Lastly, microstructure characterization and hardness testing were conducted for densified ceramic specimens.

2. Experimental Procedures

2.1 Suspension Formulation

H.C. Starck (Munich, Germany) HS B_4C powder, which has a d50 particle size range of 0.6–1.2 μm as reported by the manufacturer, was used in this study. The high specific surface area of this powder, 15–20 m^2/g as reported by the manufacturer, makes it suitable for pressureless sintering. B_4C-filled suspensions were prepared by mixing the B_4C powder with polyethylenimine (PEI) (25,000 kDa Sigma-Aldrich, St. Louis, Missouri) and deionized (DI) water. These ingredients were mixed together in a FlackTek Speedmixer DAC600.2 (Landrum, South Carolina) to produce suspensions at 50, 55, and 60 vol% solids loadings. The concentration of the PEI was 3.79 wt% relative to the B_4C content to maintain electrosteric stabilization of the suspensions (i.e., prevents the B_4C particles from settling).

For the 55 vol% B_4C suspension, MC (4,000 cP) (Sigma-Aldrich, St. Louis, Missouri) was investigated as a further stabilization agent. To prepare the MC for use, the cellulose powder was first dispersed in 70 °C DI water to make a 5 wt% suspension. The suspension was then stored overnight below 4 °C to allow for the cellulose particles to dissolve and form a gel. To form a final composition of 1 wt% MC of the DI water content of the suspension, 20 wt% of the DI water was replaced with the MC gel.

The FlackTek SpeedMixer was found to operate most effectively with viscous fluids. Therefore, the solids and liquids were gradually mixed together to keep the viscous consistency constant as the mix volume was gradually increased. Before mixing, the PEI was first dissolved in DI water. To start the batching, the MC gel was mixed with approximately 25% of the B_4C powder. The mixer was run at 800, 1200, 1600, and 2000 rpm steps at 15 s for each step. An additional 25% of the powder was then added to about a third of the PEI-DI water solution and mixed

using the same FlackTek procedure. This was repeated until all the powder and liquid was incorporated. The short, intense mixing procedure produced high shear mixing while limiting the production of heat during the mixing procedure. Long mixing times caused water evaporation due to the heat build-up.

2.2 Rheological Testing

The rheological behavior of the B_4C-filled suspensions were characterized using an Anton Paar (Graz, Austria) Modular Compact Rheometer 302 utilizing a concentric cylinder geometry. A continuous-flow viscosity curve, measuring viscosity as a function of shear rate, and an oscillatory amplitude sweep, measuring modulus as a function of shear stress at a frequency of 1 Hz, were measured for all test suspensions. As rheological properties can be heavily dependent on temperature, all tests were conducted at 25 °C to match ambient conditions during printing. After temperature stabilization, the suspensions were preconditioned by subjecting them to a shear rate of 30 s^{-1} for 1 min, followed by a 5-min relaxation period. This was conducted before each rheological test to remove the effects of shear history imparted by the sample loading.

2.3 Processing

DIW printing was conducted using a modified LulzBot Taz 6 3-D printer (Aleph Objects, Loveland, Colorado), shown in Fig. 4. This commercial system was extensively modified to accept particulate-loaded suspensions as the printing medium and deliver them volumetrically by a plunger-controlled syringe. The print head contained an internal auger for additional shear mixing and conveyance of the ceramic-filled suspensions. Details of the printer are described by Pelz et al.[9] A right-circular cylinder porous green body, 2.0 cm in diameter and 0.5 cm in height, was printed as a standard print geometry for all samples. After printing, the cylindrical samples were dried in a controlled (75.29% relative humidity) environment at room temperature for at least 24 h. The elevated humidity levels were used to reduce part cracking induced by nonuniform drying.

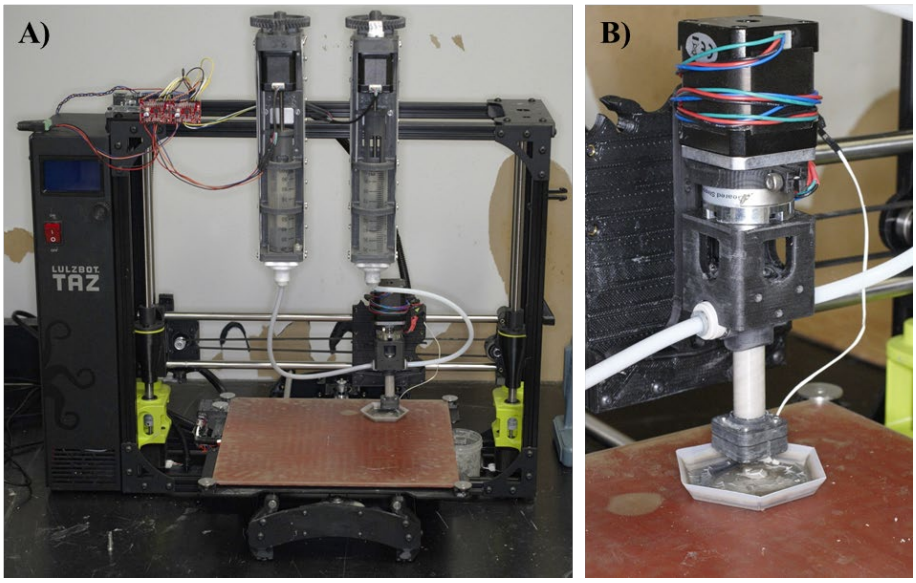

Fig. 4 Modified printer for ceramic DIW. Photographs show A) full system with dual material feed system and B) the print head containing an auger for conveyance and mixing.

Prior to sintering, binder burnout was performed on the green bodies in a flowing oxygen-gettered argon atmosphere. The furnace temperature was increased at 1 °C/min to 100 °C and held at this temperature for 3 h to remove any residual moisture. The furnace temperature was then increased at 1 °C/min to 650 °C and held for 24 h before decreasing at 3 °C/min to room temperature.

For sintering, all samples were placed into a graphite die and separated by graphite paper for sintering in an oxygen-gettered argon atmosphere (<1 ppb of oxygen). The furnace temperature was increased at 50 °C/min to 1,350 °C, held for 1 h, then increased at 50 °C/min to the sintering temperature and held for another hour. Sintering temperatures 2150 °C, 2250 °C, and 2350 °C were used in this study.

2.4 Characterization

Densities were determined using an Ax205 DeltaRange Archimedes' balance (Mettler Toledo, Columbus, Ohio). For the calculation of percent theoretical density, a value of 2.52 g/cm^3 was used for B_4C. The densified samples were cross-sectioned and mounted using EpoxySet (Allied High Tech Products, Inc., Rancho Dominguez, California) for polishing down to a 0.25-µm diamond particle suspension. Hardness testing was conducted using a diamond Knoop indentor on a Tukon 2100 hardness-testing unit (Instron, Norwood, Massachusetts) and applied 1 kgf on the cross-sectional areas of the B_4C samples following ASTM C1326-13*.

* ASTM C1326 – 13. Standard test method for Knoop indentation hardness of advanced ceramics. ASTM International; 2018.

3. Results and Discussion

As described in Section 2.1, three B_4C solid loadings of 50, 55, and 60 vol% were examined in this study. It was found that samples containing 60 vol% solids loading could not be mixed properly using the FlackTek SpeedMixer and were therefore removed from further consideration. The FlackTek operates by spinning up to 2000 rpm and mixing material at high shear rates. Most of the mixed materials flowed at the high spinning speeds and sheared along the inner wall of the container. The 60 vol% material formed a ball during spinning and resisted flow. This is believed to be because the high solids loading exceeded the critical threshold for particle jamming, creating a dilatant suspension that resisted flow.

On the other hand, samples containing 50 vol% solids loading also did not possess the rheological behavior needed for printing. When loaded into the printer feed system, the material continuously flowed under gravity with no additional pressure applied. After deposition, the yield strength of this suspension was not high enough to avoid slumping. Samples with a solids loading of 55 vol% were found to have an adequate viscosity and yield strength for printing. This difference in viscosity is highlighted in Fig. 5, demonstrating the viscosity of both samples decreasing with an increasing shear rate. This shear-thinning behavior is ideal for extrusion-type processes to prevent jamming of the nozzle. The viscosity of the suspension increased with solids loading at all shear rates for the two samples not containing MC. All further results will be reported on samples with 55 vol% solids loading.

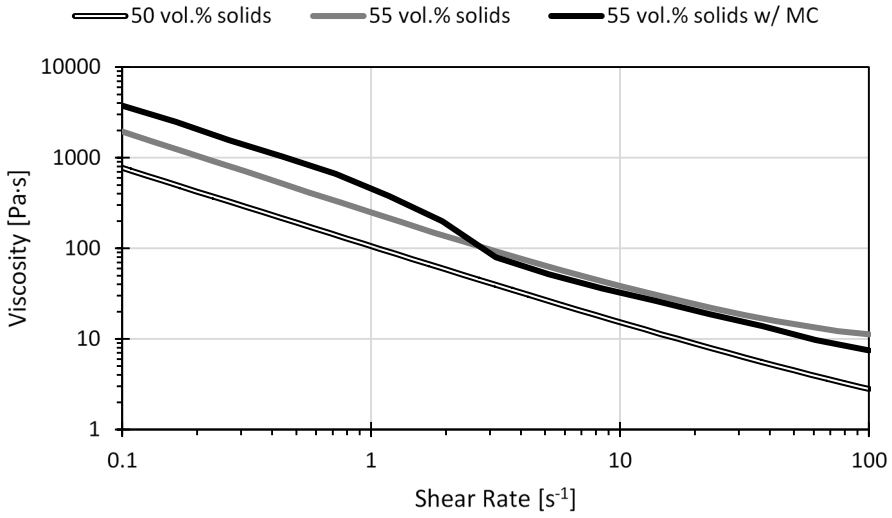

Fig. 5 Viscosity of B_4C suspensions with different ceramic content with and without MC added

The effect of MC as a rheological modifier was investigated by creating a sample at 55 vol% solids loading with 1 wt% of the liquid content replaced with MC. As seen in Fig. 5, the addition of MC to the suspension increases the viscosity at shear rates less than 2 s^{-1}. This is well below the extrusion shear rate experienced in the nozzle, as extrusion processes occur at shear rates at least an order of magnitude higher (10–1000 s^{-1}).[29] A much more significant effect of MC addition can be observed in the moduli of the suspensions, which is shown as a function of shear stress in Fig. 6. For a given shear stress, the modulus of the suspension with MC is higher than without it. Furthermore, the flow stress, or crossover point of the storage and loss modulus, is at 123 Pa for the sample without MC, and 193 Pa for the sample with MC. This higher flow stress for the suspension containing MC means the suspension can withstand higher shear before yielding and deforming. Both of these properties point to a suspension that is stiffer at low shear rates and would resist slumping after printing.

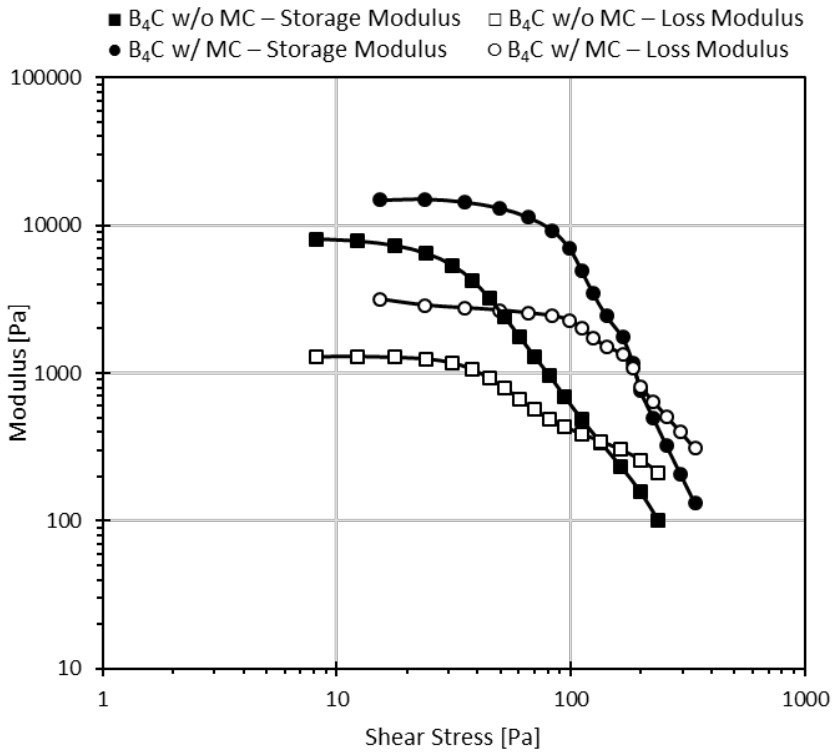

Fig. 6 Storage and loss moduli, measured at 1 Hz, of the 55 vol% B_4C suspension with and without MC added

The effect of the higher viscosity, modulus, and flow stress of the MC-containing suspensions is evident in parts printed from the two suspensions shown in Fig. 7. The edges of the sample without MC are more round and diffuse, with noticeable slumping. Conversely, on the sample containing MC, the side walls of the sample are more distinct and vertical, and the print lines of the traces are still visible.

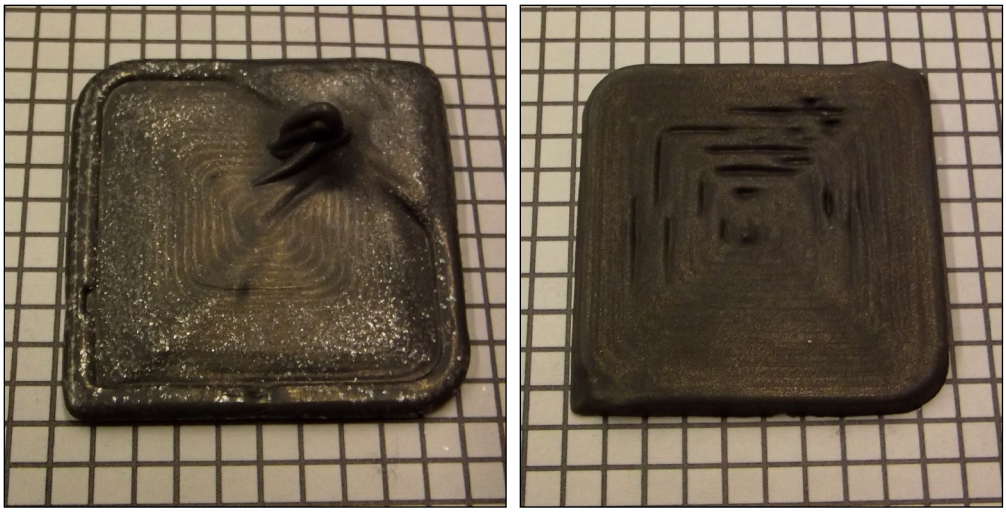

Fig. 7 Green body samples of 55 vol% B_4C suspension with (right) and without (left) MC printed by DIW (grids are 0.25 cm)

Sample densities after sintering are shown in Fig. 8. As can be seen, densities increased with increasing sintering temperature. Even at the lowest temperature investigated, the resultant density of 92.46% TD suggests the sample could be further densified using a hot isostatic postprocessing step, or sintering aids such as alumina or graphite. In addition to the highest density, significant grain growth was observed in the sample sintered at 2350 °C as shown in Fig. 9b. The pores trapped within grains indicate that complete densification cannot be achieved due to the lower rate of mass transport associated with bulk diffusion compared to grain boundary diffusion. Shrinkage of pores at grain boundaries is several orders of magnitude faster than those trapped within grains. Although higher temperatures and longer dwell times are necessary for highly dense parts, pressureless sintering provides the advantage of enabling more complex geometries that cannot conform to a die required for pressure-assisted techniques.

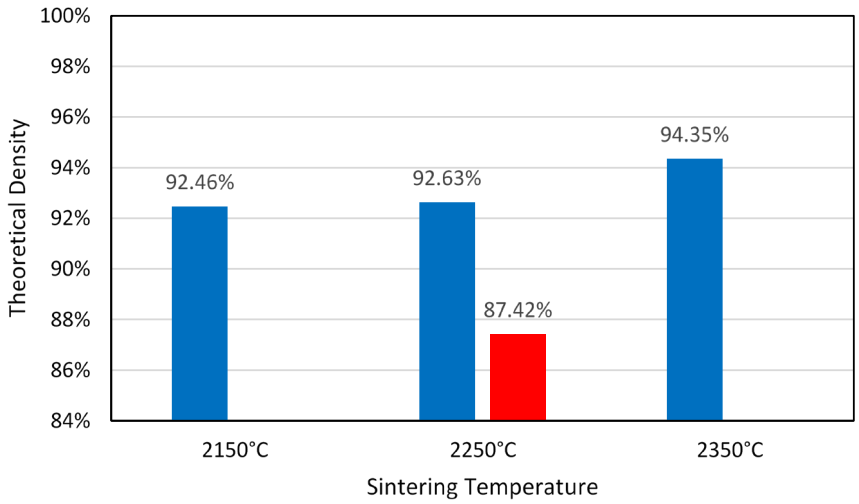

Fig. 8 Densities (%TD) of DIW B_4C samples sintered at various temperatures with (red) and without (blue) MC added

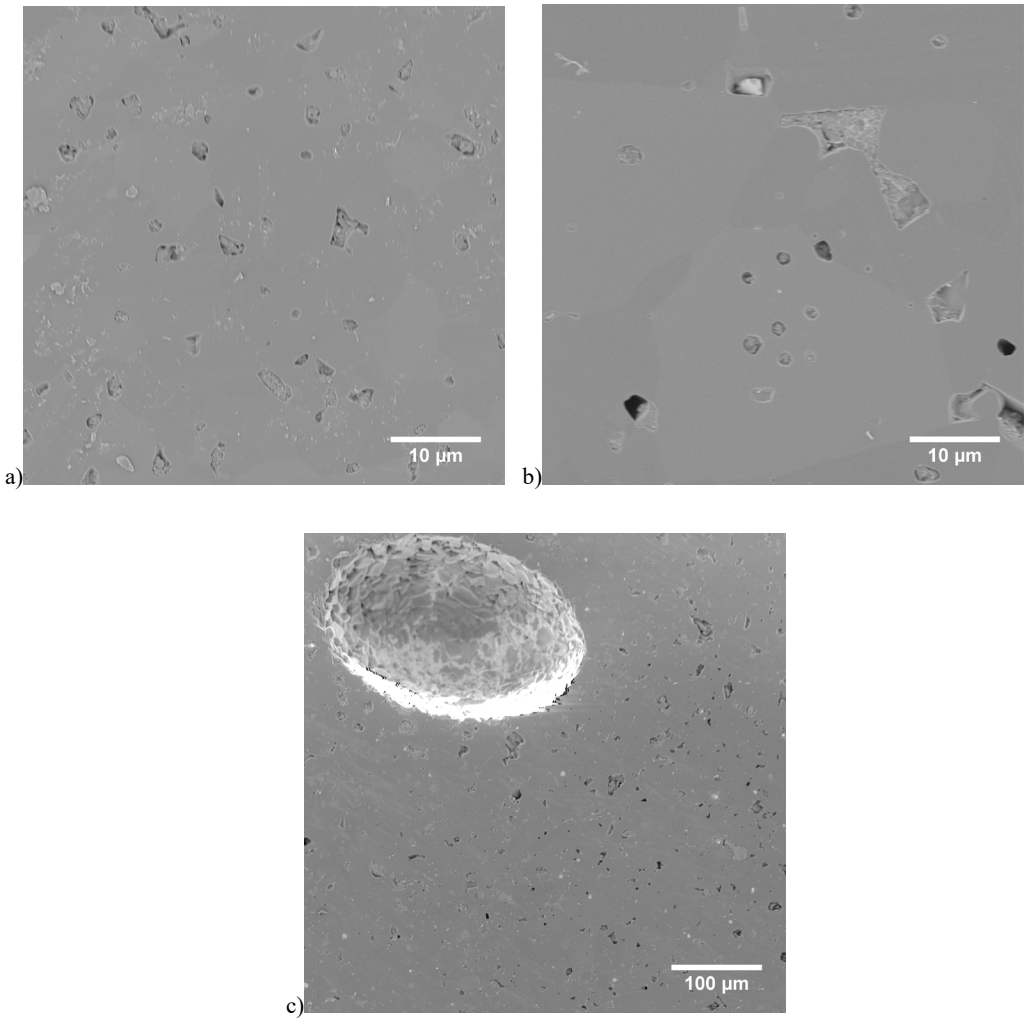

Fig. 9 Microstructure of DIW B_4C sintered at a) 2250 °C, b) 2350 °C, and c) 2250 °C with MC

Figure 9 also shows the effect of MC on sintered theoretical density. The addition of the binder decreases the sintered density by 5.2%. The microstructure of the MC sample, as shown in Fig. 9c, shows large uniformly distributed spherical pores greater than 100 μm in diameter and scattered through the sample. Due to the size and shape of the pores, it can be assumed that entrapped gas is the cause. This is likely due to the rheology of the suspension during printing, as the reduction in slumping has allowed for voids in the microstructure to remain through the DIW process. Therefore, while the MC allows for better printing of the material due to the higher viscosity and stiffer suspension, the altered rheological properties attributed to entrapped porosity within the green body during printing that remain after sintering and therefore reduce the bulk density. Another possibility is that these 100-μm pores were created during binder burnout as the result of large clumps of MC being volatilized.

For hardness testing, the B_4C samples with and without MC and sintered at 2250 °C were compared. From an average of six indents, the hardness and standard deviation were determined to be 19.16 ± 3.25 GPa for the printed sample without MC, and 19.24 ± 2.55 GPa for the sample with MC. These statistically similar hardness values indicate that processing with suspensions containing MC does not affect the intrinsic hardness of B_4C. When compared to the Knoop hardness of (fully dense) CoorsTek PAD B_4C listed at 25.5 GPa, there is a significant drop in the hardness of the material. The lower densities and associated porosity of the DIW printed pressureless sintered samples are the primary causes of this hardness difference.

4. Conclusions

A B_4C suspension with a solids loading of 55 vol% was formulated for use in DIW. The flow stress and modulus of this suspension with and without MC were measured. The addition of MC improved the rheological behavior of the suspension by increasing viscosity at low shear rates and increasing yield stress by 57%. This resulted in DIW parts that had higher-fidelity features with less slumping, but also led to lower theoretical densities of the sintered parts due to print defects in the form of large pores. The reduction in slumping is believed to contribute to pores between print traces becoming trapped in the material. This condition may potentially be alleviated by more fine-tuning of the suspension formulation and associated rheology if the pores were introduced during the DIW process.

Alternatively, if the pores were formed during the volatilization of the MC, changing burnout or sintering heating rates to allow for gas diffusion before sintering may be the solution. Heating rates of 50 °C/min were used, which may

have allowed for sintering of the microstructure before volatilized gases from the binder burnout had time to diffuse out of the powder compact. This entrapped gas could have led to the porosity in the microstructure.

Pressureless sintering of the printed samples up to 2350 °C yielded a theoretical density up to 94.35% TD. Qualitative evidence of the microstructure shows extensive grain growth, so further increasing the sintering temperature may not be the solution for decreasing porosity and increasing the final density. Nevertheless, this shows great promise as a preliminary avenue of research, as these samples contain no sintering aids to assist in densification or limit grain growth, which indicates that full density could be achieved with the incorporation of the appropriate additives. Also, a subsequent HIP process step could be used to further densify the samples. Both mechanisms offer a potential route for increased densification while maintaining complex geometries.

Hardness testing of the materials yielded 1-kgf Knoop hardness values of 19.16 and 19.24 GPa for samples with and without MC, respectively. Hardness values for samples containing MC did not significantly vary from those not containing MC. Both samples were significantly less hard than commercially available, fully dense PAD B_4C. In order to produce AM B_4C parts equivalent to traditionally manufactured materials, continued progress must be made to improve suspension formulation, including sintering aids, advanced DIW procedures to remove print defects, and improved sintering processes with the ability to fully densify the materials.

5. References

1. Thevenot F. Boron carbide—a comprehensive review. Journal of the European Ceramic society. 1990;6(4):205–25.

2. Arndt SM, Coltman JW. Design trade-offs for ceramic/composite armor materials. Advanced Materials: Looking Ahead to the 21st Century. Proceedings of 22nd International SAMPE Technical Conference. 1990. pp. 278–292.

3. Vargas-Gonzalez L, Speyer RF, Campbell J. Flexural strength, fracture toughness, and hardness of silicon carbide and boron carbide armor ceramics. International Journal of Applied Ceramic Technology. 2010;7(5):643–651.

4. Travitzky N, Bonet A, Dermeik B, Fey T, Filbert-Demut I, Schlier L, Schlordt T, Greil P. Additive manufacturing of ceramic-based materials. Advanced Engineering Materials. 2014;16(6):729–754.

5. Peng E, Zhang D, Ding J. Ceramic robocasting: recent achievements, potential, and future developments. Advanced Materials. 2018;30(47):1802404.

6. Jones TL, Vargas-Gonzalez LR, Scott B, Goodman B, Becker B. Ballistic evaluation and damage characterization of 3-D printed, alumina-based ceramics for light armor applications. International Journal of Applied Ceramic Technology. 2020;17(2):424–437.

7. Skaggs S, editor. A brief history of ceramic armor development. 27th Annual Cocoa Beach Conference on Advanced Ceramics and Composites: A: Ceramic Engineering and Science Proceedings; 2003.

8. Pelz JS, Ku N, Shoulders WT, Meyers MA, Vargas-Gonzalez LR. Multi-material additive manufacturing of functionally graded carbide ceramics via active, in-line mixing. Additive Manufacturing. 2020:101647.

9. Pelz J, Ku N, Meyers M, Vargas-Gonzalez L. Additive manufacturing utilizing a novel in-line mixing system for design of functionally graded ceramic composites. DEVCOM Army Research Laboratory; 2019. Report No.: ARL-TR-8851.

10. Li W, Martin AJ, Kroehler B, Henderson AM, Huang T, Watts JL, Hilmas G, Leu MC. Fabricating functionally graded materials by ceramic on-demand extrusion with dynamic mixing. Proceedings of the Solid Freeform Fabrication Symposium. 2018.

11. ASTM F2792-10e1. Standard A. ISO/ASTM 52900: 2015 additive manufacturing-general principles-terminology. ASTM International; 2012.

12. Griffith ML, Halloran JW. Freeform fabrication of ceramics via stereolithography. Proceedings of the Solid Freeform Fabrication Symposium. 1996.

13. Gibson I, Rosen DW, Stucker B. Additive manufacturing technologies: rapid prototyping to direct digital manufacturing. Springer; 2009.

14. Lewis JA, Smay JE, Stuecker J, Cesarano J. Direct ink writing of three-dimensional ceramic structures. Journal of the American Ceramic Society. 2006;89(12):3599–3609.

15. Cesarano J III, Baer TA, Calvert P, editors. Recent developments in freeform fabrication of dense ceramics from slurry deposition. 1997 International Solid Freeform Fabrication Symposium; 1997.

16. Cesarano J. A review of robocasting technology. Symposium V - solid freeform and additive fabrication; 1998. Vol. 542.

17. Dinger D. Rheology for ceramics. Dinger Ceramic Consulting Service; 2002. p. 213.

18. Lewis JA, Gratson GM. Direct writing in three dimensions. Materials Today. 2004;7(7–8):32–39.

19. Dudukovic NA, Wong LL, Nguyen DT, Destino JF, Yee TD, Ryerson FJ, Suratwala T, Duoss EB, Dylla-Spears R. Predicting nanoparticle suspension viscoelasticity for multimaterial 3-D printing of silica–titania glass. ACS Applied Nano Materials. 2018;1(8):4038–4044.

20. Mezger T. The rheology handbook. Curt R. Vincentz Verlag Hannover; 2002.

21. M'barki A, Bocquet L, Stevenson A. Linking rheology and printability for dense and strong ceramics by direct ink writing. Scientific Reports. 2017;7(1):1–10.

22. Rueschhoff L, Costakis W, Michie M, Youngblood J, Trice R. Additive manufacturing of dense ceramic parts via direct ink writing of aqueous alumina suspensions. International Journal of Applied Ceramic Technology. 2016;13(5):821–830.

23. Rahaman MN, Xiao W. Three-dimensional printing of Si3N4 bioceramics by robocasting. Advanced Ceramics and Composites. 2017;38(2):235.

24. Cai K, Román-Manso B, Smay JE, Zhou J, Osendi MI, Belmonte M, et al. Geometrically complex silicon carbide structures fabricated by robocasting. Journal of the American Ceramic Society. 2012;95(8):2660–2666.

25. Costakis WJ Jr, Rueschhoff LM, Diaz-Cano AI, Youngblood JP, Trice RW. Additive manufacturing of boron carbide via continuous filament direct ink writing of aqueous ceramic suspensions. Journal of the European Ceramic Society. 2016;36(14):3249–3256.

26. Cho N, Bao Z, Speyer RF. Density-and hardness-optimized pressureless sintered and post-hot isostatic pressed B_4C. Journal of Materials Research. 2005;20(8):2110–2116.

27. Jones TL, Vargas-Gonzalez L, Scott B, Goodman B, Becker B. An in-depth analysis of competing 3-D printed methods for the mobile manufacturing of body armor at the point of need. DEVCOM Army Research Laboratory; 2019. Report No.: ARL-TR-8684.

28. Swab JJ. Recommendations for determining the hardness of armor ceramics. International Journal of Applied Ceramic Technology. 2004;1(3):219–225.

29. Reed JS. Principles of ceramics processing. Wiley; 1995.

List of Symbols, Abbreviations, and Acronyms

AM	additive manufacturing
B_4C	boron carbide
DI	deionized
DIW	direct-ink write
HIP	hot isostatic pressing
MC	methylcellulose
PAD	pressure-assisted densified
PEI	polyethylenimine
ppb	parts per billion
TD	theoretical density
UV	ultraviolet

1 (PDF) DEFENSE TECHNICAL INFORMATION CTR DTIC OCA

1 (PDF) DEVCOM ARL
FCDD RLD DCI
TECH LIB

82 (PDF) DEVCOM ARL
FCDD RLR
D STEPP
FCDD RLR E
C VARANASI
FCDD RLR EM
M BAKAS
E RUNNERSTROM
FCDD RLW
J ZABINSKI
A RAWLETT
S SCHOENFELD
FCDD RLW B
C HOPPEL
L VARGAS-GONZALEZ
R BECKER
J CAMPBELL
P GILLICH
A TONGE
FCDD RLW D
E ROBINETTE
B MCWILLIAMS
FCDD RLW M
B CHEESEMAN
E CHIN
K CHO
W ROY
FCDD RLW MA
J SANDS
E WETZEL
FCDD RLW MB
C FOUNTZOULAS
G GAZONAS
J LIGDA
B LOVE
D MAGAGNOSC
J PITTARI
B POWERS
J SIETINS
Z WILSON
FCDD RLW MC
S WALCK
FCDD RLW MD
J LA SCALA
S WALSH
FCDD RLW ME
K BEHLER
V BLAIR
R BRENNAN
S COLEMAN
A DIGIOVANNI
J DUNN
M GOLT
M GUZIEWSKI
S HIRSCH
C HUBBARD
M IVILL
S KILCZEWSKI
M KORNECKI
N KU
J LASALVIA
T PARKER
P PATEL
S RAJU
A ROSENBERGER
W SHOULDERS
S SILTON
J SWAB
FCDD RLW MF
P GOINS
C HAINES
E HERNANDEZ
E HORWATH
FCDD RLW MG
J LENHART
R MROZEK
E NAPADENSKY
FCDD RLW PB
J MCDONALD
S SATAPATHY
T WEERASOORIYA
FCDD RLW PC
J CAZAMIAS
D CASEM
J CLAYTON
R LEAVY
J LLOYD
C MEREDITH
T SCHARF
C WILLIAMS
FCDD RLW PD
R DONEY
K STOFFEL
FCDD RLW LH
P JANNOTTI
L MAGNESS
D MALICK
FCDD-RLW-PE
C KRAUTHAUSER
P SWOBODA
FCDD RLW S
J CIEZAK-JENKINS
A WEST

5 DEVCOM SC
(PDF) FCDD SCP
J KIREJCZYK
FCDD SCP WI
R DILALLA
A FOURNIER
C LEWIS
FCDD SCP WP
D PHELPS

1 PEO SOLDIER
(PDF) SFAE SDR SPIE
D OTTERSON